Generation of vibrational modes via ferromagnetic resonance

Author: Sergio Jiménez Torrejón
Facultat de Física, Universitat de Barcelona, Diagonal 645, 08028 Barcelona, Spain.

Advisor: Dr. Joan Manel Hernàndez Ferràs

Abstract: This work presents the study of a thin film of yttrium iron garnet (YIG) deposited on a gadolinium gallium garnet (GGG) substrate using ferromagnetic resonance (FMR) measurements, with the aim of analyze the magnon-phonon coupling under resonant conditions. Based on the study of the absorbed energy S_{21}, as a function of frequency and magnetic field, a periodic structure following the FMR resonance profile has been observed. The analysis reveals that the periodicity is consistent with a stationary phonon mode in the GGG substrate. Finally, the magnetic properties of the sample have been determined.

Keywords: Solid State Physics, Magnetism, Ferromagnetic Resonance and Phonons
SDGs: 4. Quality education and 9. Industry, innovation and infrastructure

I. INTRODUCTION

Ferromagnetic resonance (FMR) is a technique that enables the study and characterization of the magnetic properties of ferromagnetic materials. It consists of applying a static magnetic field and, perpendicularly, an oscillating magnetic field that induces the precession of the magnetic moments. Resonance occurs when the frequency of the oscillating field matches the precession frequency of the magnetic moments; this is known as the resonance frequency or the *Larmor* frequency. At resonance, the magnetic moments absorb energy from the oscillating field, which is dissipated through *spin-orbit* interactions, spin-phonon interactions within the material, *spin-flips*...

The collective excitations of the spins can be described in terms of quasiparticles known as magnons, which represent spin waves, i.e., the quantum excitations of magnetization.

Phonons, the quantized excitations of elastic waves in solids, can couple weakly to magnons via magnetoelastic interaction. However, recent studies [1–3] have shown that in systems composed of a high-quality acoustic resonator and a magnetic material with strong *spin-orbit* interaction, this coupling can become significant. Under resonance conditions, magnetic energy can leak into the acoustic resonator via *phonon pumping*, which leads to an increase in magnetic damping with non-linear frequency dependence [3].

The aim of this work is to determine the magnetic properties of a single layer of *yttrium iron garnet* (YIG) deposited on a *gadolinium gallium garnet* (GGG) substrate, as well as to observe and analyze the magnon-phonon coupling in the YIG/GGG sample using FMR measurements.

II. THEORETICAL MODEL

This section provides a brief explanation and theoretical demonstration of ferromagnetic resonance dynamics.

When a magnetic field $\mathbf{B}_0$ is applied to a single electron, a torque is exerted on its magnetic moment $\mathbf{m}$: $\Gamma = m \times B_0$; which, using $\Gamma = \mathrm{d}l/\mathrm{d}t$, leads to:

$$\frac{\mathrm{d}\mathbf{m}}{\mathrm{d}t} = \gamma(\mathbf{m} \times \mathbf{B}_0) \tag{1}$$

where γ is the gyromagnetic ratio. Considering that the field is oriented along the z-direction, the torque causes the magnetic moment to precess around the field direction with the *Larmor* frequency $f_L = \gamma B_0/2\pi$.

A ferromagnet can be classically treated as a macrospin. Applying a sufficiently strong static magnetic field B_0 causes most domains to align in the same direction; thus, a uniform magnetization, M, can be assumed. To observe resonance, a high-frequency magnetic field $\mathbf{b}_1$ is applied perpendicular to $\mathbf{B}_0$. Then, analogously to the single electron case and assuming absence of damping:

$$\frac{\mathrm{d}\mathbf{M}}{\mathrm{d}t} = \gamma(\mathbf{M} \times \mathbf{B}_0) \tag{2}$$

It follows that the magnetization precesses around the field axis with *Larmor* frequency $f_0 = \gamma B_0/2\pi$. In ferromagnets, must be taken into account the external field $\mathbf{B}$ and the internal field $\mathbf{B}' = \mathbf{B} + \mathbf{B}_d$, where $\mathbf{B}_d$ = -$\mathcal{N}\mathbf{M}/\mu_0$, and $\mathcal{N}$ is the demagnetizing tensor (assumed to be diagonal).

Since $b_1 \ll B_0$, the magnetization can be expressed as $\mathbf{M} \approx M_s\mathbf{e}_z + \mathbf{m}(\mathrm{t})$, where $\mathbf{m}(\mathrm{t})$ is the oscillating component in the x-y plane. Then, using Eq. (2) and the aforementioned external and internal fields, Kittel's expression [4, 5] for the resonant frequency is obtained:

$$f_0^2 = \gamma^2 \left[B_0 + (\mathcal{N}_x - \mathcal{N}_z)\,\mu_0 M\right]\left[B_0 + (\mathcal{N}_y - \mathcal{N}_z)\,\mu_0 M\right] \quad (3)$$

Considering a thin film and applying a field $\mathbf{B}_0$ in the plane:

$$f_0 = \frac{\gamma}{2\pi}\sqrt{B_0\,(B_0 + \mu_0 M_s)} \quad (4)$$

where M_s is the saturation magnetization. Equation Eq. (4) describes the dependence of the resonance frequency f_0 on the applied field B_0.

The perpendicular field $\mathbf{b}_1$ causes the spins to precess at a certain frequency; as this frequency approaches the resonant f_0, the system begins to absorb energy from the excitation. Once resonance is reached, the energy is dissipated (mainly in form of heat) due to the damping process.

Magnetic anisotropy also plays an important role and can be incorporated into the Kittel's equation adding an anisotropy field B_a to B_0.

Finally, although theoretical models for magnetic and elastic coupling are still under development, it has been established [1, 6, 7] that the interaction between phonons and magnons behaves as two coupled harmonic oscillators with discrete frequencies. The interaction is described by the magnetoelastic coupling g_{me} as [6]; the frequencies for each quasiparticles are: f_m for the magnetic mode, described by Eq. (4), and f_p for the elastic mode.

In this context, phonons propagate through the substrate with a wavelength corresponding to half of the thickness of the GGG: $\lambda = t_{GGG}/2$. This implies that the characteristic frequency is given by

$$f_\mathrm{p} = \frac{v}{2t_\mathrm{GGG}}\ , \quad (5)$$

where v is the speed of sound in GGG.

III. EXPERIMENTAL PROCEDURE

The sample analyzed in this work is a thin magnetic film of yttrium iron garnet (YIG) with a thickness of 1 μm, deposited on a non-magnetic substrate of gadolinium gallium garnet (GGG) with a thickness of 550 μm.

The experimental setup consists of: an electromagnet with its current supply, the YIG/GGG sample, a vector network analyzer (VNA), a coplanar waveguide, microwave cables and a Hall probe.

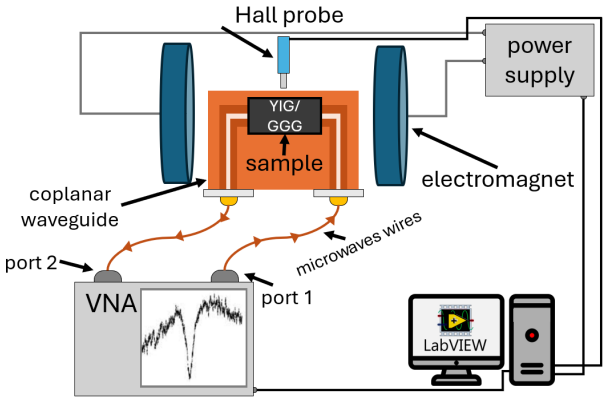

FIG. 1: Illustration of the experimental setup for FMR.

The VNA is a device that sends microwave signals through port 1 and receives them through port 2. It enables the visualization, for each transmitted frequency, of the ratio between the sent and the received signal, i.e., the signal loss profile.

The coplanar waveguide consists of a conductive trace patterned on a dielectric substrate. It propagates the microwaves sent by the VNA.

To perform the FMR study, a static magnetic field is applied using the electromagnet; the sample is placed between the poles of the magnet on top of the coplanar waveguide. The VNA sends microwaves through the microwave cable connected to port 1, which reaches the coplanar waveguide, generating a high-frequency oscillating magnetic field perpendicular to the static field applied by the electromagnet. Finally, the transmitted waves are collected at port 2 of the VNA. The intensity of the collected signal is represented by the S_{21} parameter, expressed in decibel units (dB) as directly provided by the VNA; see Fig. 1.

The experimental setup is controlled using a *LabView* program. This allows setting the range of intensities applied to the electromagnet from the power supply and the range of frequencies sent by the VNA. For each applied current the VNA performs a frequency sweep and the measured $S_{21}(f)$ is sent to the PC. The program returns a data file containing the applied current, the corresponding magnetic fields measured by the Hall probe, the frequency and the received signal S_{21}. Under resonance conditions a peak in S_{21} intensity should be observed corresponding to the absorption of energy.

Finally, it is important to highlight the relevance and the reason for using a YIG/GGG sample. YIG is one of the magnetic materials with the lowest known *spin-wave damping factor*; which enables obtaining very sharp FMR peaks. Furthermore, the anisotropy of the sample is very small since both YIG and GGG have highly perfect

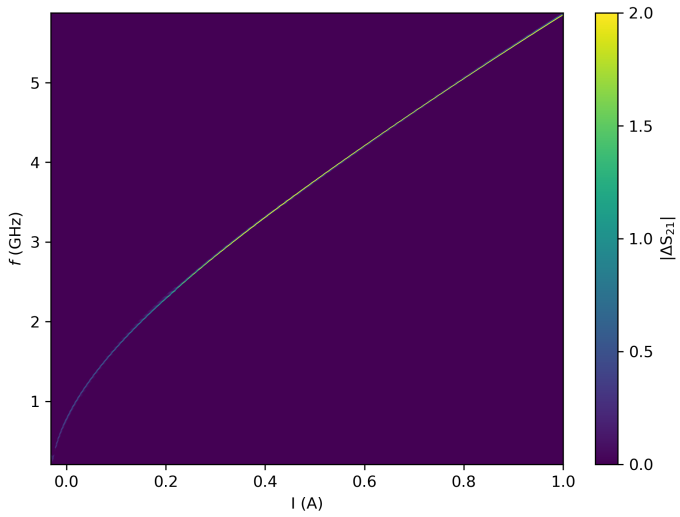

FIG. 2: Map of S_{21} for each intensity applied to the electromagnet and frequency sent by the VNA.

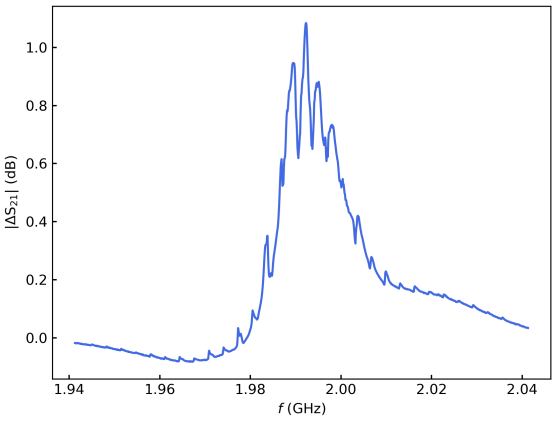

FIG. 3: $|\Delta S_{21}|$ vs frequency f for a fixed applied current $I = 0.1504$ A.

crystal structures and are very well lattice-matched at their interface. The low anisotropy allows to consider Eq. (4) as a first approximation. All of these properties favor good propagation of magnons and phonons, making it possible to perform a very precise study of their coupling.

IV. EXPERIMENTAL RESULTS AND ANALYSIS

An FMR measurement on the YIG/GGG sample was performed by measuring S_{21} over a current range from –0.03 A to 0.22 A with steps of 0.003 A, and in a frequency range from 417 MHz to 5870 MHz with steps of 0.1 MHz, see Fig. 2. The analysis is performed in terms of current, which is linearly proportional to the magnetic field within the considered range, with known conversion factors. The $S_{21}(I, f)$ values corresponding to resonance (those that clearly stand out from the background) follow the typical Kittel-like $f(B)$ profile: Eq. (4). At first glance, is not observed any phonon interaction. However, plotting a cut of S_{21} vs frequency f at a fixed magnetic field shows the coupling phenomena, see Fig. 3.

The S_{21} values as a function of frequency or intensity follow a Lorentzian profile, two examples are shown in Fig. 3 and Fig. 4. In addition to the Lorentzian shape in the frequency dependence of S_{21}, small regularly spaced peaks are observed; these correspond to phonon interactions. Moreover, the peak intensity increases as their position approaches the resonance center.

With these data, the objective is to precisely determine the frequency of the elastic mode f_p and extract the magnetic properties of the sample.

Observation of Magnon-Phonon Coupling

The absorbed energy increases under resonance conditions, as previously discussed, and when magnon–phonon interaction is present it becomes larger compared to the case without such interaction. Therefore, the frequency of the elastic mode f_p can be extracted from the energy response. It should be noted that the analysis yields the spacing between characteristic frequencies: Δf_p, not the fundamental frequency f_p directly.

For a fixed frequency, S_{21} is plotted as a function of the applied current (which corresponds to the magnetic field H), see Fig. 4. Then, for each frequency is calculated the integral of S_{21} over the applied current range:

$$A(f) = \int_{I_{min}}^{I_{max}} \Delta S_{21}(I, f) \; \mathrm{d}I \tag{6}$$

The area $A(f)$ is modulated by the magnon–phonon interaction. As in the case of two coupled oscillators, interference effects can be constructive or destructive; hence, the area will be correspondingly larger or smaller.

The integrated signal $A(f)$ exhibits large periodic oscillations with a frequency Δf_{setup}, as shown in Fig. 5. These oscillations are attributed to resonances from the measurement hardware itself. From the figure, the setup frequency can be estimated as $\Delta f_{\text{setup}} \approx 0.06$ GHz.

So, in Fig. 5, the envelope area reflects the setup resonance, while the superimposed oscillations are attributed to periodic coupling between magnons and elastic modes. In order to isolate the phonon interaction in $A(f)$, a smoothing filter is applied, so only the setup behavior is retained. The difference between the smoothed curve and the experimental area is $\Delta A(f)$,

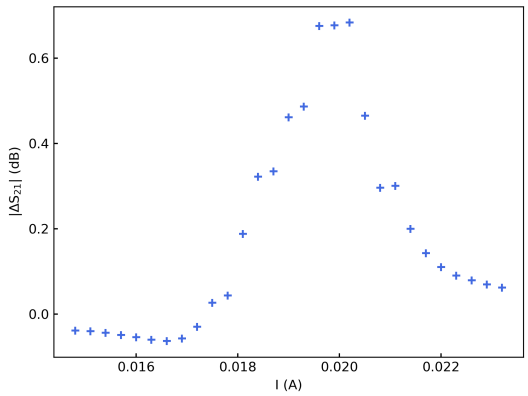

FIG. 4: $|\Delta S_{21}|$ vs intensity for $f = 1000.2$ MHz.

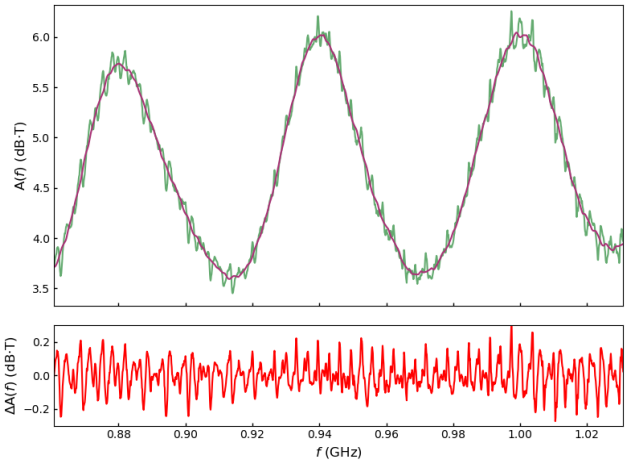

FIG. 5: Integrated signal A(f) as a function of frequency f (green), and also plotted with a smoothing filter applied (brown). ΔA(f) corresponds to the difference between the two areas.

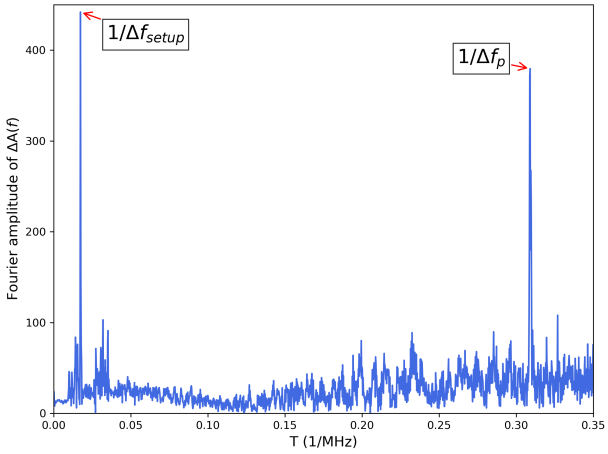

FIG. 6: Fourier spectrum of the differential signal $\Delta A(f)$ in the period domain T.

reveals the contribution from magnon–phonon coupling.

Once the phonon interaction is isolated, the Fourier transform of the difference ΔA(f) is computed to extract the periodicity (see Fig. 6). From this analysis is obtained the setup frequency: $\Delta f_{setup} = 57.458$ MHz and the resulting periodicity of the elastic mode:

$$\Delta f_{\mathrm{p}} = 3.235 \pm 0.006 \text{ MHz}$$

The obtained value can be compared using Eq. (5). The thickness of the GGG substrate lies around $t_{\mathrm{GGG}} \approx 550$ μm and the transverse sound velocity for GGG is $v_t = 3570$ m/s [1]; hence, the corresponding frequency is $\Delta f_{\mathrm{p}} \approx 3.245$ MHz. The value is very similar to the experimentally obtained one, likely due to the high-quality lattice matching and flatness structure of GGG. Moreover, this result is consistent with values reported in other studies using YIG/GGG samples of similar dimensions [3, 8].

Characterization of Magnetic Properties

Finally, the magnetic properties of the material have been characterized: the gyromagnetic ratio γ and the saturation magnetization M_s.

The resonance frequency and magnetic field values follow the form of Eq. (4). Therefore, the resonance frequency is plotted as a function of the effective field B_c and fitted to Eq. (4) to extract γ and M_s. The effective field B_c is calculated as the weighted average of the magnetic field using the S_{21} intensity as weight:

$$B_c \equiv \langle B \rangle = \frac{\int_{B_{min}}^{B_{max}} \Delta \mathrm{S}_{21}\,(B, f) \cdot B \text{ dB}}{\int_{B_{min}}^{B_{max}} \Delta \mathrm{S}_{21}\,(B, f) \text{ dB}} \qquad (7)$$

From the fit of the experimental data in Fig. 7 to Eq. (4), the values $\gamma/2\pi = 27.696 \pm 0.005$ GHz/T and $\mu_0 M_s = 0.1959 \pm 0.0001$ T are obtained. The obtained gyromagnetic ratio $\gamma/2\pi$ is in good agreement with those reported by other studies [1, 9, 10].

The large-scale behavior of magnons follows the typical Kittel-like profile, while the phonon mode remains fixed at Δf_{p}. At the intersection of the two modes, a clear anticrossing is observed, as shown in Fig. 7(a); this is characteristic of the coupling between two oscillators and indicates strong hybridization between the modes. These small peaks result from magnon–phonon coupling, with a characteristic separation Δf_{p}; in agreement with the frequency determined from the Fourier transform of ΔA(f). Additionally, in Fig. 7(b) oscillations due to the

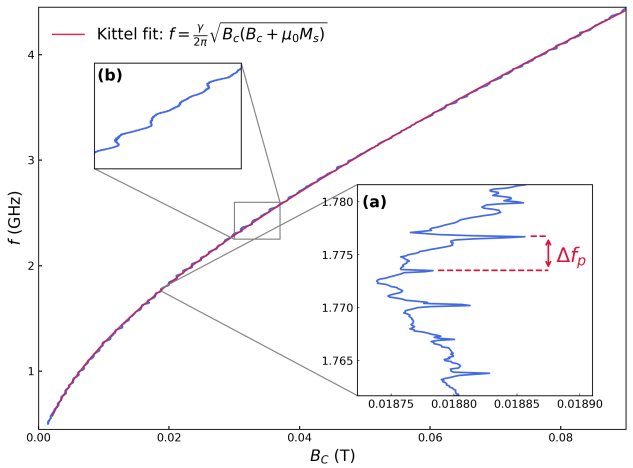

FIG. 7: Frequency f as a function of the effective field B_c, with a typical Kittel-like $f(B)$ fit. (a) Zoom of the resonance region around $f \approx 1.70$ GHz is shown; the separation between frequency peaks is $\Delta f_{\mathrm{p}} \approx 3.24$ MHz. (b) Zoom of an intermediate frequency region around $f \approx 2.4$ GHz.

experimental setup with characteristic frequency $\Delta f_{\mathrm{setup}}$ are observed.

V. CONCLUSIONS

In this work, a film of yttrium iron garnet (YIG) deposited on a gadolinium gallium garnet (GGG) substrate has been studied. Through ferromagnetic resonance (FMR) measurements, the magnon–phonon coupling was analyzed and the magnetic properties of the sample were determined.

Firstly, the frequency of the elastic mode was calculated via the absorbed S_{21} signal and its frequency spectrum: $\Delta f_{\mathrm{p}} = 3.235 \pm 0.002$ MHz. This frequency matches the expected frequency of a phonon mode confined within the GGG substrate with a wavelength $\lambda = 2t_{\mathrm{GGG}}$; and it is also consistent with other studies using similar YIG/GGG samples.

Finally, by fitting the experimental values of the resonance frequency f as a function of the effective field B_c using the typical Kittel-like profile, the effective saturation magnetization was extracted as $\mu_0 M_s = 0.1959 \pm 0.0001$ T and the gyromagnetic ratio as $\gamma/2\pi = 27.696 \pm 0.005$ GHz/T; both in excellent agreement with values reported in the literature.

This study confirms the relevance of magnetoelastic interaction in high-quality YIG/GGG systems providing clear evidence of strong magnon-phonon coupling under resonant conditions.

Acknowledgments

I would like to personally thank my advisor, Dr. Joan Manel Hernàndez Ferràs, for all his support, encouragement, guidance and patience throughout this work. I would also like to thank my family and friends for their patience in listening to me talk endlessly about magnons and phonons for months.

[1] R. Schlitz, L. Siegl, T. Sato, W. Yu, G. E. W. Bauer, H. Huebl, and S. T. B. Goennenwein, *Magnetization dynamics affected by phonon pumping*, Phys. Rev. B 106, 014407 (2022).

[2] M. Müller, J. Weber, F. Engelhardt, V. A. S. V. Bittencourt, T. Luschmann, M. Cherkasskii, M. Opel, S. T. B. Goennenwein, S. Viola Kusminskiy, S. Geprägs, R. Gross, M. Althammer, and H. Huebl, *Chiral phonons and phononic birefringence in ferromagnetic metal–bulk acoustic resonator hybrids*, Phys. Rev. B 109, 024430 (2024).

[3] S. Streib, H. Keshtgar, and G. E.W. Bauer, *Damping of Magnetization Dynamics by Phonon Pumping*, Phys. Rev. Lett. 121, 027202 (2018).

[4] C. Kittel, *Introduction to Solid State Physics*, 8th ed. (John Wiley & Sons, New York, 2005), Chap. 10, pp. 160–185.

[5] J. M. D. Coey, *Magnetism and Magnetic Materials* (Cambridge University Press, Cambridge, 2010), Chap. 9.

[6] A. Litvinenko, R. Khymyn, V. Tyberkevych, V. Tikhonov, A. Slavin, and S. Nikitov, *Tunable Magnetoacoustic Oscillator with Low Phase Noise*, Phys. Rev. Appl. 15, 034057 (2021).

[7] S. Probst, F. B. Song, P. A. Bushev, A. V. Ustinov, and M. Weides, *Tunable Magnetoacoustic Oscillator with Low Phase Noise*, Rev. Sci. Instrum. 86, 024706 (2015).

[8] K. An, A. N. Litvinenko, R. Kohno, A. A. Fuad, V. V. Naletov, L. Vila, U. Ebels, G. de Loubens, H. Hurdequint, N. Beaulieu, J. Ben Youssef, N. Vukadinovic, G. E. W. Bauer, A. N. Slavin, V. S. Tiberkevich, and O. Klein, *Coherent long-range transfer of angular momentum between magnon Kittel modes by phonons*, Phys. Rev. B 101, 060407(R) (2020).

[9] D. Cheshire, P. Bencok, D. Gianolio, G. Cibin, V. K. Lazarov, G. van der Laan, S. A. Cavill *Absence of spin-mixed states in ferrimagnet yttrium iron garnet*, J. Appl. Phys. **132**, 103902 (2022).

[10] Seongjae Lee, Scott Grudichak, Joseph Sklenar, C. C. Tsai, Moongyu J., Qinghui Yang, Huaiwu Z., John B. Ketterson, *Ferromagnetic resonance of a YIG film in the low frequency regime*, J. Appl. Phys. **120**, 033905 (2016).

Generació de modes vibracionals via ressonància ferromagnètica

Author: Sergio Jiménez Torrejón
Facultat de Física, Universitat de Barcelona, Diagonal 645, 08028 Barcelona, Spain.

Advisor: Dr. Joan Manel Hernàndez Ferràs

Resum: En aquest treball s'ha estudiat una monocapa fina de *yttrium iron garnet* (YIG) depositada sobre un substrat de *gadolinium gallium garnet* (GGG) mitjançant mesures de ressonància ferromagnètica (FMR), amb l'objectiu d'analitzar l'acoblament entre magnons i fonons en condicions de ressonància. A partir del tractament de la intensitat del senyal S_{21}, segons la freqüència i el camp magnètic, s'ha observat una certa periodicitat que segueix el perfil de ressonància d'FMR. De l'anàlisi s'ha obtingut que la periodicitat és consistent amb un mode fonònic estacionari del substrat de GGG. Per acabar, s'han determinat les propietats magnètiques de la mostra.

Paraules clau: Física d'Estat Sòlid, Magnetisme, Ressonància Ferromagnètica i Fonons.
ODSs: 4. Educació de qualitat i 9. Indústria, innovació, infraestructures.

Objectius de Desenvolupament Sostenible (ODSs o SDGs)

1. Fi de la es desigualtats		10. Reducció de les desigualtats	
2. Fam zero		11. Ciutats i comunitats sostenibles	
3. Salut i benestar		12. Consum i producció responsables	
4. Educació de qualitat	X	13. Acció climàtica	
5. Igualtat de gènere		14. Vida submarina	
6. Aigua neta i sanejament		15. Vida terrestre	
7. Energia neta i sostenible		16. Pau, justícia i institucions sòlides	
8. Treball digne i creixement econòmic		17. Aliança pels objectius	
9. Indústria, innovació, infraestructures	X		

Aquest TFG, com a part del Grau de Física, s'inscriu dins l'Objectiu de Desenvolupament Sostenible (ODS) número 4, relacionat amb una educació de qualitat; i més concretament amb la meta 4.4, ja que fomenta la formació i l'aprenentatge en l'àmbit universitari. També es relaciona amb l'ODS 9, concretament amb la fita 9.5, ja que l'estudi de l'acoblament magnó-fonó potencia la recerca en tecnologies més eficients basades en dispositius de FMR.

GRAPHICAL ABSTRACT